
Is ^{18}F -3'-Fluoro-3'-Deoxy-L-Thymidine Useful for the Staging and Restaging of Non-Small Cell Lung Cancer?

David C.P. Cobben, PhD^{1,2}; Philip H. Elsinga, PhD¹; Harald J. Hoekstra, PhD²; Albert J.H. Suurmeijer, PhD³; Willem Vaalburg, PhD¹; Bram Maas, BSc¹; Pieter L. Jager, PhD¹; and Harry M.J. Groen, PhD⁴

¹PET Center, Groningen University Hospital, Groningen, The Netherlands; ²Department of Surgical Oncology, Groningen University Hospital, Groningen, The Netherlands; ³Department of Pathology and Laboratory Medicine, Groningen University Hospital, Groningen, The Netherlands; and ⁴Department of Pulmonary Diseases, Groningen University Hospital, Groningen, The Netherlands

The objective of this study was to compare ^{18}F -3'-fluoro-3'-deoxy-L-thymidine (FLT) PET with clinical TNM staging, including that by ^{18}F -FDG PET, in patients with non-small cell lung cancer (NSCLC). **Methods:** Patients with NSCLC underwent whole-body ^{18}F -FDG PET and whole-body ^{18}F -FLT PET, using a median of 360 MBq of ^{18}F -FDG (range, 160–500 MBq) and a median of 210 MBq of ^{18}F -FLT (range, 130–420 MBq). ^{18}F -FDG PET was performed 90 min after ^{18}F -FDG injection, and ^{18}F -FLT PET was performed 60 min after ^{18}F -FLT injection. Two viewers independently categorized the localization and intensity of tracer uptake for all lesions. All ^{18}F -FDG PET and ^{18}F -FLT PET lesions were compared. Staging with ^{18}F -FLT PET was compared with clinical TNM staging based on the findings of history, physical examination, bronchoscopy, CT, and ^{18}F -FDG PET. From 8 patients, standardized uptake values (SUVs) were calculated. Maximal SUV and mean SUV were calculated. **Results:** Sixteen patients with stage IB–IV NSCLC and 1 patient with strong suspicion of NSCLC were investigated. Sensitivity on a lesion-by-lesion basis was 80% for the 8 patients who received treatment before ^{18}F -FLT PET and 27% for the 9 patients who did not receive pretreatment, using ^{18}F -FDG PET as the reference standard. Compared with clinical TNM staging, staging by ^{18}F -FLT PET was correct for 8 of 17 patients: 5 of 9 patients in the group with previous therapy and 3 of 8 patients in the group without previous therapy. The maximal SUV of ^{18}F -FLT PET, at a median of 2.7 and range of 0.8–4.5, was significantly lower than that of ^{18}F -FDG PET, which had a median of 8.0 and range of 3.7–18.8 ($n = 8$; $P = 0.012$). The mean SUV of ^{18}F -FLT PET, at a median of 2.7 and range of 1.4–3.3, was significantly lower than that of ^{18}F -FDG PET, which had a median of 6.2 and range of 2.8–13.9 ($n = 6$; $P = 0.027$). **Conclusion:** ^{18}F -FLT PET is not useful for staging and restaging NSCLC.

Key Words: ^{18}F -FLT; ^{18}F -FDG; non-small cell lung cancer; clinical TNM staging; PET

J Nucl Med 2004; 45:1677–1682

Received Feb. 29, 2004; revision accepted Apr. 29, 2004.
For correspondence or reprints contact: David C.P. Cobben, MD, PET Center, University of Groningen Hospital, P.O. Box 30.001, 9700 RB Groningen, The Netherlands.
E-mail: D.C.P.Cobben@pet.azg.nl

PET, using ^{18}F -FDG, has been accepted as a noninvasive metabolic imaging method for the staging of lung cancer (1). ^{18}F -FDG uptake reflects glucose consumption (2). However, ^{18}F -FDG is not a selective tracer, since it also accumulates in inflammatory cells. For instance, macrophages invade tumors and appear in inflammatory lesions, causing false-positive ^{18}F -FDG PET results (3–5). Another problem is decreased uptake during hyperglycemia (6). Furthermore, because avidly taken up by the brain, ^{18}F -FDG PET lacks sensitivity for imaging brain metastases.

In the search for more specific PET tracers, ^{18}F -fluoro-3'-deoxy-3'-L-fluorothymidine (FLT) has been developed by Shields and Grierson. ^{18}F -FLT may not have these drawbacks (7,8). This pyrimidine analog is phosphorylated by the enzyme thymidine kinase 1, which leads to intracellular trapping (8). Enzyme thymidine kinase 1 concentration increases almost tenfold during DNA synthesis, and ^{18}F -FLT uptake may therefore accurately reflect cellular proliferation (9).

Few data are available on the clinical comparison of ^{18}F -FLT with ^{18}F -FDG for staging and restaging of non-small cell lung cancer (NSCLC) (10–12). The aim of the study was to compare ^{18}F -FLT PET with clinical TNM staging in patients with NSCLC, including ^{18}F -FDG PET.

MATERIALS AND METHODS

Patients

In this prospective study, patients with histologically or cytologically confirmed NSCLC who attended the outpatient department for various treatments were included. For all patients, disease was staged according to the TNM system before ^{18}F -FLT PET (13). Clinical TNM staging was based on the findings of patient history, physical examination, bronchoscopy, chest radiography, CT, and ^{18}F -FDG PET. All patients had been or were to be included in chemotherapy or radiotherapy protocols at the time of the inclusion. Organ functions such as those of liver, kidney, and bone marrow had to be within normal limits. Pregnant patients and patients with psychiatric disorders were excluded. The Medical

Ethics Committee of the Groningen University Hospital approved the study protocol. All patients gave written informed consent.

Tracer Synthesis

^{18}F -FLT was synthesized according to the method of Machulla et al. (14). ^{18}F -FLT was produced by ^{18}F -fluorination of the 4,4'-dimethoxytrityl-protected anhydrothymidine, followed by a deprotection step. After purification by reversed-phase high-performance liquid chromatography, the product was made isotonic and passed through a 0.22- μm filter. ^{18}F -FLT was produced with a radiochemical purity of >95% and specific activity of >10 TBq/mmol. ^{18}F -FDG was synthesized according to the method of Hamacher et al. by an automated synthesis module (15).

PET

All ^{18}F -FLT PET scans were attenuation corrected and obtained on an ECAT EXACT HR+ (Siemens/CTI Inc.). Nine ^{18}F -FDG PET scans were attenuation corrected and obtained on an ECAT EXACT HR+. The remaining 8 ^{18}F -FDG PET scans were non-attenuation corrected, of which 4 were obtained on an ECAT EXACT HR+ and 4 on an ECAT 951/31. It is our experience that the difference between the 2 cameras and between the use of attenuation-corrected and non-attenuation-corrected technique for ^{18}F -FDG PET is negligible for staging NSCLC. Because ^{18}F -FLT was the experimental tracer and our experience with ^{18}F -FLT in lung cancer was limited, we used only attenuation-corrected images obtained with the EXACT HR+ camera. Patients were instructed to fast for at least 6 h before undergoing PET. They also were instructed to drink 1 L of water before being imaged, to stimulate ^{18}F -FLT and ^{18}F -FDG excretion from the renal calyces. For injection of the radiopharmaceuticals, a venous cannula was inserted into the forearm of the patient. From this cannula, a 2-mL blood sample was taken to measure the serum glucose level before each ^{18}F -FDG PET scan. The median interval between ^{18}F -FDG PET and ^{18}F -FLT PET was 3 d, and the range was 1–63 d. Patients were injected with a median of 360 MBq of ^{18}F -FDG (range, 160–500 MBq) and a median of 210 MBq of ^{18}F -FLT (range, 130–420 MBq). Ninety minutes after ^{18}F -FDG injection and 60 min after ^{18}F -FLT injection, interleaved attenuation-corrected whole-body scanning was performed from crown to femur, with 3 and 5 min allowed per bed position for transmission and emission scanning, respectively. Data from multiple bed positions were iteratively reconstructed (ordered-subsets expectation maximization) into attenuated and nonattenuated ^{18}F -FLT and ^{18}F -FDG whole-body PET images (16).

Data Analysis

Two experienced PET physicians evaluated the ^{18}F -FLT PET images independently and were unaware of patients' clinical information, including ^{18}F -FDG PET findings. The observers ranked the intensity of uptake in each lesion in comparison with background uptake in the lungs. The intensity was ranked as 0 (no visible uptake), 1 (slight increase in uptake), 2 (moderate increase in uptake), or 3 (strong increase in uptake). The observers reached a consensus on a lesion-by-lesion basis according to the same intensity scale for differently scored lesions. Thereafter, lesions ranked as 0 or 1 were grouped as hypo- or normometabolic lesions and lesions that ranked as 2 or 3 were grouped as hypermetabolic lesions.

To compare the staging properties of ^{18}F -FLT PET with those of the clinical TNM system, the presence or absence of pulmonary, mediastinal, and distant hypermetabolic lesions was used. The

mediastinal lesions were assigned according to the Mountain and Dresler classification of regional lymph nodes (17). The exact location of N1 and N2 lesions is difficult to assess on PET, and these lesions were therefore read in conjunction with CT after all PET scans had been evaluated. Lesions outside the mediastinum were described according to their anatomic locations.

After analysis of the lesions and the staging properties, standardized uptake value (SUV) was calculated from the attenuation-corrected ^{18}F -FDG PET and ^{18}F -FLT PET scans. The visually most hypermetabolic lesion on ^{18}F -FLT PET images of each patient was compared with the corresponding lesion on transaxial ^{18}F -FDG PET sections. The slice with the highest uptake was selected for ROI analysis. After selecting the plane with the maximum SUV, an ROI was drawn manually. ROIs were placed at the 70% contour of the maximal SUV in the tumor when possible. In other cases, ROIs were drawn manually. The SUVs of ^{18}F -FLT PET and ^{18}F -FDG PET were compared. Images were displayed on a Sun Microsystems workstation. ROI calculation was performed with Clinical Applications Programming Package (version 5; CTI).

Statistical Analysis

The degree of interobserver agreement for detection of ^{18}F -FLT PET and ^{18}F -FDG PET lesions was quantified with κ -statistics. For analyses of the intensity of each lesion, the values from the consensus readings were used. Sensitivity was calculated on a lesion level, using the number of pulmonary, mediastinal, and distant hypermetabolic lesions. Sensitivity is expressed as mean, with 95% coincidence interval (CI). Staging properties of ^{18}F -FLT PET based on the presence or absence of pulmonary, mediastinal (expressed as N1 and N2 lesions), or distant hypermetabolic lesions were compared with the clinical TNM staging system. The Wilcoxon signed-rank test was used to compare maximal SUV and mean SUV between ^{18}F -FDG PET and ^{18}F -FLT PET. Two-tailed P values < 0.05 were considered significant.

RESULTS

Patients

From January 2002 until March 2003, 17 consecutive patients were included in this study. Their characteristics are shown in Table 1. Nine patients were included for primary staging and 8 patients were included for restaging. Seven of the restaged patients completed therapy before undergoing PET. Patient 3 was scanned during chemotherapy, because of clinical progression. All patients had histologically confirmed tumors, with the exception of patient 17, who had no malignancy but was included because of strong suspicion of malignancy. Primarily, histologic confirmation was difficult to obtain in this patient and therefore PET was performed to get more information.

Accuracy of ^{18}F -FLT PET

^{18}F -FLT PET produced easily interpretable images (Fig. 1). Most prominent physiologic uptake of the tracer was observed in liver, bone marrow, intestines, and bladder. Negligible and uniform tracer uptake was observed in the lungs. No uptake of tracer was observed in the brain, mediastinum, or myocardium.

TABLE 1
Patient Characteristics and Detectability of Hypermetabolic Lesions on ¹⁸F-FLT PET as Compared with Standard ¹⁸F-FDG PET

Patient no.	Age (y)	Sex	Histology	TNM	Stage	Previous therapy	Interval between treatment and PET	Consensus ¹⁸ F-FDG result				Consensus ¹⁸ F-FLT result			
								TL	N1	N2	D	TL	N1	N2	D
Patients with pretreatment															
1	57	F	AC	T2 N2-3 M1	IV	Cisplatin and gemcitabine	27 mo	4	1	4	2	1	1	2	2*
2	56	F	AC	T2 N3 M1	IV	Docetaxel	14 mo	1	0	1	3*	2	0	0	3*
3	64	F	AC	T4 N0 M1	IV	Cisplatin and gemcitabine and second-line paclitaxel and docetaxel	Just before third cycle of docetaxel	2	0	0	1	1	0	0	0
4	58	M	SCC	T4 N1 M1	IV	Epirubicin and gemcitabine	9 mo	1	1	0	1	1	0	0	0
5	62	M	LCUC	T4 N2 M0	IIIB	Cisplatin and gemcitabine	17 mo	1	0	0	0	1	0	0	0
6	54	F	AC	T4 N2 M1	IV	Cisplatin and gemcitabine and second-line docetaxel and irinotecan	1 mo	4	0	1	11*	2	0	1	2
7	45	M	SCC	T1 N0 M1	IV	Radiotherapy on abdomen (in 1983), mediastinum (in 1983), and head and neck and supraclavicular region (in 2000)	20 mo	0	0	0	2	0	0	0	1
8	61	M	SCC	T2 N2 M1	IV	Radiotherapy on recurrent tumor	2 mo	1	0	1	1*	0	0	0	1
9	53	M	AC	Tx N2/3 M1	IV	Radiotherapy on acetabulum	1 wk	5	0	1	30*	0	0	0	0
Patients without pretreatment															
10	57	M	SCC	T2 N0 M0	IB	None	NA	1	0	0	0	1	0	0	0
11	70	M	SCC	T2 N2 M0	IIIA	None	NA	1	0	1	0	0	1	1	0
12	67	M	SCC	T4 N0 M1	IV	None	NA	1	0	0	1*	1	0	0	1*
13	73	M	SCC	T4 N2 M0	IIIB	None	NA	1	0	0	0	1	0	0	1
14	74	M	SCC	T4 N2 M0	IIIB	None	NA	0	0	3	0	0	0	3	1
15	65	M	LCUC	T4 N2 M1	IV	None	NA	1	1	1	1*	1	0	0	0
16	43	F	AC	T4 N2 M1	IV	None	NA	2	0	3	2	1	1	2	0
17	52	M	NM	NM		None	NA	0	0	0	0	0	0	0	0
Total								26	3	16	55	13	3	9	12

*Including pulmonary lesions located outside the lobe containing the primary tumor.

TL = lesions in lungs; N1 = lesions located at N1 node; N2 = lesions located at N2; D = distant hypermetabolic lesions; AC = adenocarcinoma; SCC = squamous cell carcinoma; LCUC = large cell undifferentiated carcinoma; NA = not applicable; NM = no malignancy.

Interobserver agreement for the detection of lesions (κ) was 0.51 (SE = 0.06) for ¹⁸F-FLT PET and 0.55 (SE = 0.06) for ¹⁸F-FDG PET.

The overall sensitivity of ¹⁸F-FLT PET for the detection of all hypermetabolic lesions was 37% (95% CI, 29%–45%), compared with detection of those lesions on ¹⁸F-FDG PET (Table 2). The sensitivity of ¹⁸F-FLT PET for the detection of pulmonary, mediastinal (expressed as N1 and N2 lesions), and distant hypermetabolic lesions was, respectively, 50% (95% CI, 34%–66%), 56% (95% CI, 37%–75%), and 21% (95% CI, 12%–30%) using ¹⁸F-FDG PET as the reference standard. Sensitivity was calculated on a lesion-by-lesion basis for ¹⁸F-FLT PET using ¹⁸F-FDG PET as the reference standard. In the 8 patients without pretreatment, sensitivity was 80% (95% CI, 67%–93%), and in the 9 patients with pretreatment, sensitivity was 27% (95% CI, 3%–51%).

Compared with clinical TNM staging, staging by ¹⁸F-FLT PET was correct for 8 of 17 patients (Table 1): 5 of 9 patients in the group with previous therapy and 3 of 8 patients in the group without previous therapy.

Uptake of ¹⁸F-FDG was significantly higher than that of ¹⁸F-FLT, when expressed as maximal SUV and mean SUV. Maximal SUV was a median of 2.7 (range, 0.8–4.5) for

¹⁸F-FLT PET and a median of 8.0 (range, 3.7–18.8) for ¹⁸F-FDG PET ($n = 8$; $P = 0.012$). Mean SUV was a median of 2.7 (range, 1.4–3.3) for ¹⁸F-FLT PET and a median of 6.2 (range, 2.8–13.9) for ¹⁸F-FDG PET ($n = 6$; $P = 0.027$).

Additional ¹⁸F-FLT PET Findings

In patient 11, CT showed a T1 tumor suggestive of malignancy in the right upper lobe. On both ¹⁸F-FDG PET and ¹⁸F-FLT PET, mediastinal hypermetabolic lesions were detected (Fig. 1). On ¹⁸F-FDG PET and CT, the primary tumor was located within an area suggestive of postobstructive inflammation. On ¹⁸F-FDG PET, this area showed diffuse ¹⁸F-FDG uptake. In contrast, this inflammation was not visible on ¹⁸F-FLT PET, as could be expected. Patient 9 was treated with radiation therapy of the acetabulum. The field of radiation therapy and the remnant of the metastasis showed slightly decreased ¹⁸F-FLT activity. This lesion was ranked as hypometabolic, because the observers were unaware of the clinical history of the patient (Fig. 2). On ¹⁸F-FDG PET, this area appeared as a hypermetabolic lesion, although one must bear in mind that this appearance could have been caused by locally increased uptake in inflammatory tissue (Fig. 2). Patient 4 demonstrated a photopenic defect in the liver, which corresponded to a pho-

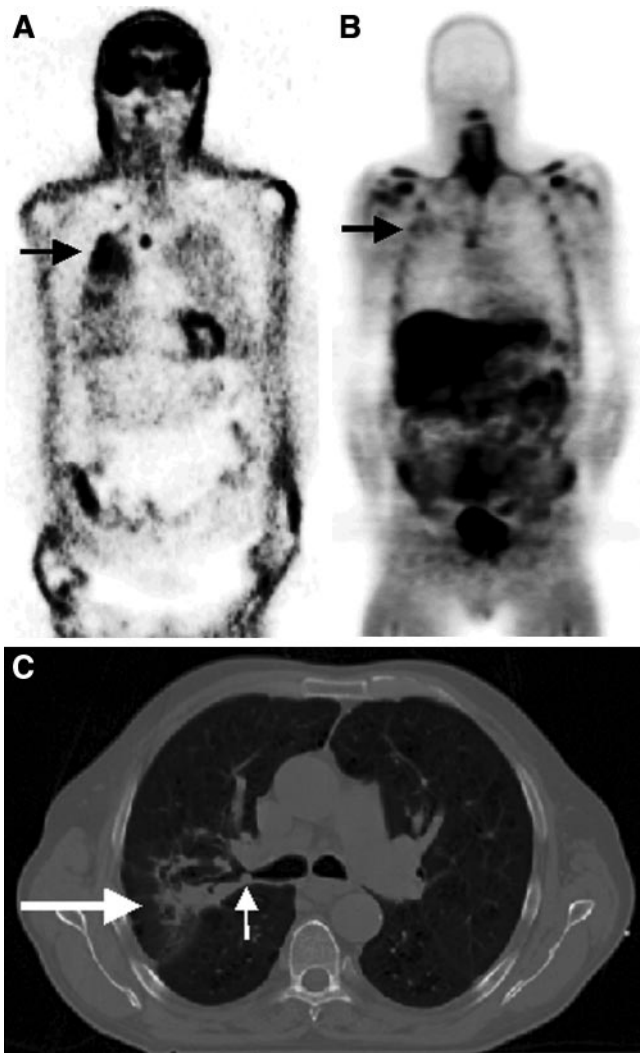


FIGURE 1. Coronal ^{18}F -FDG PET image (A), ^{18}F -FLT PET image (B), and CT image (C) of patient 11, diagnosed with squamous cell carcinoma in the right upper bronchus (small white arrow) and distally with suspected postobstruction pneumonia (large white arrow) on CT. Avid uptake of ^{18}F -FDG can be seen in a pretracheal lesion and in the primary tumor, which is in an area of elevated uptake, probably postobstructive pneumonia (black arrow). Less avid uptake of ^{18}F -FLT can be seen in the area of the tumor, and little ^{18}F -FLT uptake can be seen in the suspected infected area (black arrow). The bone marrow of ribs and the shoulder bones, liver, and intestine show physiologic ^{18}F -FLT uptake.

topenic defect in a hypermetabolic liver lesion on ^{18}F -FDG PET (Fig. 3). Vital tumor tissue in the margin cannot be discriminated from the surrounding tissue because of the high physiologic ^{18}F -FLT uptake in the liver. This lesion was suspected to be a liver metastasis seen on CT.

DISCUSSION

Despite the potential of ^{18}F -FLT for imaging proliferation of cancer, our results indicate that ^{18}F -FLT is inferior to ^{18}F -FDG for staging NSCLC. This finding is consistent with

TABLE 2
Maximum and Mean SUV and Wilcoxon
Nonparametric Test

Patient no.	Lesion	^{18}F -FLT		^{18}F -FDG	
		Maximum SUV, tumor	Mean SUV, tumor	Maximum SUV, tumor	Mean SUV, tumor
1	M	4.5	3.3	9.9	6.9
2	P	3.0	2.4	9.2	7.3
3	P	1.6	NA	6.7	5.4
4	P	3.9	3.1	18.8	13.9
10	P	3.1	2.9	10.0	7.8
13	P	0.8	NA	5.4	4.4
14	M	2.4	1.9	5.1	3.7
16	P	1.8	1.4	3.7	2.8

M = mediastinal lesion; P = pulmonary lesion; NA = not assessable.

findings reported in 2 recently published abstracts and 1 article (10–12).

This study focused on the staging properties of ^{18}F -FLT PET in patients with (foremost) disseminated NSCLC. The sensitivity of mediastinal and distant hypermetabolic lesions was low, resulting in incorrect staging in 9 of 17 patients (5 in the group that received pretreatment and 4 in the group that did not). Most of the visible ^{18}F -FLT lesions were categorized as less intense than the comparable lesions on

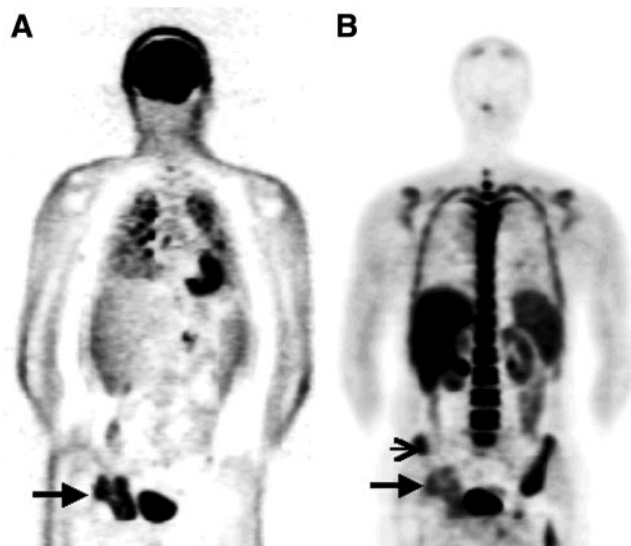


FIGURE 2. Coronal ^{18}F -FDG PET image (A) and ^{18}F -FLT PET image (B) of patient 9, with multiple lesions in both lungs on ^{18}F -FDG PET and no lesions on ^{18}F -FLT PET. Metastasis in the right acetabulum, which had been irradiated 1 wk earlier, is prominent on ^{18}F -FDG PET (large arrow) but less intense on ^{18}F -FLT PET (large arrow). In addition, irradiated bone marrow cranial of tumor has become metabolically inactive, as is seen on ^{18}F -FLT as uptake less intense than that in nonirradiated bone marrow (small arrow).

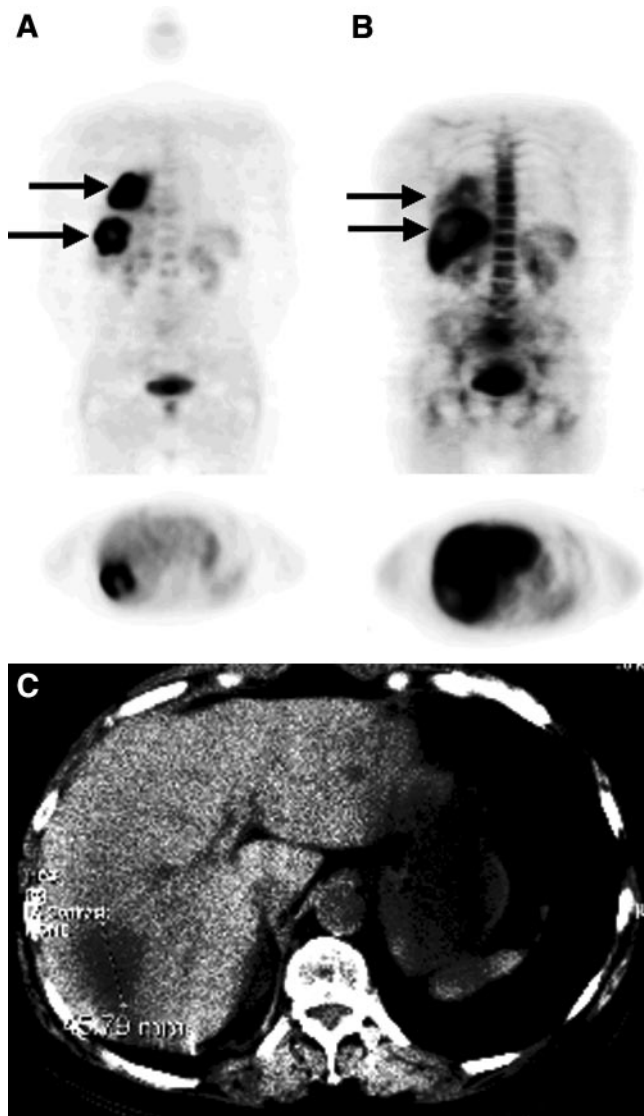


FIGURE 3. Coronal and transaxial ^{18}F -FDG PET (A), ^{18}F -FLT PET (B), and CT (C) images of patient 4, diagnosed with a large tumor in the right lower lung and a large metastasis in the liver (large arrows on PET images). The liver metastasis, with a 4.5-cm diameter, can be seen on CT. ^{18}F -FDG PET showed avid uptake in the lung tumor and liver metastasis, whereas ^{18}F -FLT uptake was slightly less in the pulmonary lesion and almost absent in the liver metastasis.

^{18}F -FDG PET. Other studies have confirmed that ^{18}F -FLT PET is not an accurate tracer for staging NSCLC (10–12).

^{18}F -FLT uptake is related to cellular proliferation, whereas ^{18}F -FDG uptake is related to increased glucose metabolism. Because most cancer cells are metabolically active but fewer cells are proliferating, a higher net uptake of ^{18}F -FDG than of ^{18}F -FLT in the tumor can be expected. Besides tumor cells, many inflammation cells are usually present in malignant lesions, resulting in a higher ^{18}F -FDG uptake than ^{18}F -FLT uptake (3). Moreover, it is known that the ^{18}F -FLT phosphorylation rate in vitro is about 30% of the phosphorylation rate of serum thymidine by thymidine

kinase 1, possibly explaining the low ^{18}F -FLT uptake in the tumor (18,19). In this study, of a small and heterogeneous group of patients, the maximal SUV of ^{18}F -FLT ranged from 0.8 to 4.5, compared with 3.7 to 18.8 for ^{18}F -FDG. Vesselle et al. also found low ^{18}F -FLT uptake, with maximal SUVs ranging from 0.9 to 6.9 (20); Buck et al. found maximal SUVs ranging from 1.3 to 10.4 (12). Lesions with a low SUV can increase the risk for misinterpretation and thus influence the accuracy of staging with ^{18}F -FLT PET.

Other mechanisms might explain the low sensitivity of ^{18}F -FLT PET for the detection of NSCLC lesions. One explanation in this study could be that 9 patients received chemotherapy or radiation therapy before undergoing PET. The effects of chemotherapy on ^{18}F -FLT uptake have been studied in vitro and in vivo in animals. These studies were performed on esophageal cells 24 and 72 h after treatment with 4 different types of chemotherapy and on mice with fibrosarcoma 24 and 48 h after treatment with 5-FU (21,22). The studies showed that the increase or decrease of ^{18}F -FLT uptake in the tumor after chemotherapy depends on the type of chemotherapy. However, no clinical data are available to explain the decreased uptake of ^{18}F -FLT in NSCLC patients with progression after first- and second-line chemotherapy. In the 8 patients who did not receive previous therapy, the results for staging were also poor, concordant with the preliminary results of Yap et al., who found a poor sensitivity for ^{18}F -FLT PET in untreated NSCLC patients as well (10). On one hand, a decrease of ^{18}F -FLT after therapy could be a major advantage for ^{18}F -FLT PET over ^{18}F -FDG PET and should not be interpreted per se as a lack of sensitivity. On the other hand, the group of pretreated patients showed clinical progression of disease, indicating a lower sensitivity for ^{18}F -FLT PET. The ideal situation would be to obtain pathologic confirmation of the lesions, to correlate the cellular activity with ^{18}F -FLT uptake.

CONCLUSION

Our study indicated that not only pulmonary lesions but also mediastinal and distant metastatic lesions are not well identified by ^{18}F -FLT PET. Therefore, staging with ^{18}F -FLT PET in patients with NSCLC is not recommended.

ACKNOWLEDGMENTS

This research was funded by Dutch Cancer Foundation grant 2000-2299.

REFERENCES

- Pieterman RM, van Putten JW, Meuzelaar JJ, et al. Preoperative staging of non-small-cell lung cancer with positron-emission tomography. *N Engl J Med.* 2000;343:254–261.
- Herholz K, Rudolf J, Heiss WD. FDG transport and phosphorylation in human gliomas measured with dynamic PET. *J Neurooncol.* 1992;12:159–165.
- Kubota R, Yamada S, Kubota K, Ishiwata K, Tamahashi N, Ido T. Intratumoral distribution of fluorine-18-fluorodeoxyglucose in vivo: high accumulation in macrophages and granulation tissues studied by microautoradiography. *J Nucl Med.* 1992;33:1972–1980.
- Yamada Y, Uchida Y, Tatsumi K, et al. Fluorine-18-fluorodeoxyglucose and

- carbon-11-methionine evaluation of lymphadenopathy in sarcoidosis. *J Nucl Med.* 1998;39:1160–1166.
5. Strauss LG. Fluorine-18 deoxyglucose and false-positive results: a major problem in the diagnostics of oncological patients. *Eur J Nucl Med.* 1996;23:1409–1415.
 6. Langen KJ, Braun U, Rota KE, et al. The influence of plasma glucose levels on fluorine-18-fluorodeoxyglucose uptake in bronchial carcinomas. *J Nucl Med.* 1993;34:355–359.
 7. Mier W, Haberkorn U, Eisenhut M. [(18)F]FLT: portrait of a proliferation marker. *Eur J Nucl Med.* 2002;29:165–169.
 8. Shields AF, Grierson JR, Dohmen BM, et al. Imaging proliferation in vivo with [F-18]FLT and positron emission tomography. *Nat Med.* 1998;4:1334–1336.
 9. Sherley JL, Kelly TJ. Regulation of human thymidine kinase during the cell cycle. *J Biol Chem.* 1988;263:8350–8358.
 10. Yap CS, Schiepers C, Quon A, et al. A comparison between [F-18]fluorodeoxyglucose (FDG) and [F-18]3'-deoxy-3'-fluorothymidine (FLT) uptake in solitary pulmonary nodules and lung cancer [abstract]. *J Nucl Med.* 2003;44(suppl):123P.
 11. Buck AK, Hetzel M, Schirmeister H, et al. [(18)F]FLT and [(18)F]FDG-PET for assessment of pulmonary nodules [abstract]. *Eur J Nucl Med.* 2003;29(suppl):S121.
 12. Buck AK, Halter G, Schirmeister H, et al. Imaging proliferation in lung tumors with PET: (18)F-FLT versus (18)F-FDG. *J Nucl Med.* 2003;44:1426–1431.
 13. Sobin L, Wittekind C. *TNM Classification of Malignant Tumours.* 6th ed. New York, NY: John Wiley & Sons; 2002:97–103.
 14. Machulla HJ, Blochter A, Kuntzsch M, Piert M, Wei R, Grierson JR. Simplified labeling approach for synthesizing 3'-deoxy-3'-[(18)F]fluorothymidine [(18)F]FLT). *J Radioanalytical Nucl Chem.* 2000;243:843–846.
 15. Hamacher K, Coenen HH, Stocklin G. Efficient stereospecific synthesis of no-carrier-added 2-[(18)F]-fluoro-2-deoxy-D-glucose using aminopolyether supported nucleophilic substitution. *J Nucl Med.* 1986;27:235–238.
 16. Lonnew M, Borbath I, Bol A, et al. Attenuation correction in whole-body FDG oncological studies: the role of statistical reconstruction. *Eur J Nucl Med.* 1999;26:591–598.
 17. Mountain CF, Dresler CM. Regional lymph node classification for lung cancer staging. *Chest.* 1997;111:1718–1723.
 18. Munch-Petersen B, Cloos L, Tyrsted G, Eriksson S. Diverging substrate specificity of pure human thymidine kinases 1 and 2 against antiviral dideoxynucleosides. *J Biol Chem.* 1991;266:9032–9038.
 19. Toyohara J, Waki A, Takamatsu S, Yonekura Y, Magata Y, Fujibayashi Y. Basis of FLT as a cell proliferation marker: comparative uptake studies with [3H]thymidine and [3H]arabinothymidine, and cell-analysis in 22 asynchronously growing tumor cell lines. *Nucl Med Biol.* 2002;29:281–287.
 20. Vesselle H, Grierson J, Muzi M, et al. In vivo validation of 3'-deoxy-3'-[(18)F]fluorothymidine ([18F]FLT) as a proliferation imaging tracer in humans: correlation of [(18)F]FLT uptake by positron emission tomography with Ki-67 immunohistochemistry and flow cytometry in human lung tumors. *Clin Cancer Res.* 2002;8:3315–3323.
 21. Dittmann H, Dohmen BM, Kehlbach R, et al. Early changes in [(18)F]FLT uptake after chemotherapy: an experimental study. *Eur J Nucl Med Mol Imaging.* 2002;29:1462–1469.
 22. Barthel H, Cleij MC, Collingridge DR, et al. 3'-deoxy-3'-[(18)F]Fluorothymidine as a new marker for monitoring tumor response to antiproliferative therapy in vivo with positron emission tomography. *Cancer Res.* 2003;63:3791–3798.

